bergen, S.; Holden, D. A.; Marchessault, R. H. *Polym. Prepr. (Am. Chem. Soc., Div. Polym. Chem.)* **1988**, *29* (1), 594.
(6) Gross, R. A.; DeMello, C.; Lenz, R. W.; Brandl, H.; Fuller, R. C. *Macromolecules* **1989**, *22*, 1106.
(7) Brandl, H.; Gross, R. A.; Lenz, R. W.; Fuller, R. C. *Appl. Environ. Microbiol.* **1988**, *54*, 1977.
(8) Gross, R. A.; Brandl, H.; Ulmer, H. W.; Posada, M. A.; Fuller, R. C.; Lenz, R. W. *Polym. Prepr. (Am. Chem. Soc., Div. Polym. Chem.)* **1989**, *30* (1), 492.
(9) Brandl, H.; Gross, R. A.; Knee, E. J.; Lenz, R. W.; Fuller, R. C. *Int. J. Appl. Biol.* **1989**, *11*, 49.
(10) Doi, Y.; Kunioka, M.; Tamaki, A. *Polym. Prepr. (Am. Chem. Soc., Div. Polym. Chem.)* **1988**, *29* (1), 588.
(11) Holmes, P. A. *Phys. Technol.* **1985**, *16*, 32.
(12) Lavallee, C.; Grenier, D.; Prud'homme, R. E.; Le Borgne, A.; Spassky, N. In *Advances in Polymer Synthesis*; Culbertson, B. M., McGrath, J. E., Eds.; Plenum: New York, 1985; p 450.
(13) Seebach, D.; Roggo, S.; Zimmermann, J. In *Stereochemistry of Organic and Bioorganic Transformations*; Bartmann, W., Sharpless, K. B., Eds.; VCH: Weinheim, West Germany, 1987; Vol. 17, pp 7-126.
(14) Iida, M.; Hayase, S.; Araki, T. *Macromolecules* **1978**, *11*, 490.
(15) Gross, R. A.; Zhang, Y.; Konrad, G.; Lenz, R. W. *Macromolecules* **1988**, *21*, 2657.
(16) Agostini, D. E.; Lando, J. B.; Shelton, J. R. *J. Polym. Sci., Part A-1* **1971**, *9*, 2775.
(17) Teranishi, K.; Iida, M.; Araki, T.; Yamashita, S.; Tani, H. *Macromolecules* **1974**, *7*, 421 and references therein.
(18) Iida, M.; Araki, T.; Teranishi, K.; Tani, H. *Macromolecules* **1977**, *10*, 275.
(19) Le Borgne, A.; Spassky, N. *Polym. Prepr. (Am. Chem. Soc., Div. Polym. Chem.)* **1988**, *29* (1), 598.
(20) Shelton, J. R.; Lando, J. B.; Agostini, D. E. *J. Polym. Sci., Part B* **1971**, *9*, 173.
(21) Shelton, J. R.; Agostini, D. E.; Lando, J. B. *J. Polym. Sci., Part A-1* **1971**, *9*, 2789.
(22) Kricheldorf, H. R.; Berl, M.; Scharnagl, N. *Macromolecules* **1988**, *21*, 286.

# Morphological Characterization of Bioerodible Polymers. 1. Crystallinity of Polyanhydride Copolymers

**Edith Mathiowitz, Eyal Ron, George Mathiowitz,† Carmela Amato, and R. Langer***

*Department of Chemical Engineering, Massachusetts Institute of Technology, Cambridge, Massachusetts 02139*

*Received October 6, 1989; Revised Manuscript Received December 20, 1989*

ABSTRACT: The composition of polyanhydrides has been a critical determinant in enabling different erosion rates of these polymers. Since crystallinity is an important factor in controlling polymer erosion rates, an in-depth analysis of the effect of polymer composition on crystallinity was undertaken using a variety of polyanhydrides. Polyanhydride homopolymers and copolymers made of sebacic acid (SA), (carboxyphenoxy)propane (CPP), (carboxyphenoxy)hexane (CPH), and fumaric acid (FA) were studied. Crystallinity was analyzed by the following: (1) X-ray diffraction, (2) a combination of X-ray diffraction and differential scanning calorimetry (DSC), and (3) data generated from $^1$H NMR spectroscopy and Flory's equilibrium theory. Homopolymers such as poly(sebacic anhydride), poly(fumaric anhydride), and poly(1,3-bis(*p*-carboxyphenoxy)propane anhydride) were crystalline, and each displayed a typical powder diffraction. In copolymers, diffraction patterns were determined, in most cases, by the monomer of highest concentration. Copolymers with high ratios of SA or CPP had a high crystallinity while copolymers with almost equal ratios of SA and CPP or SA and CPH were amorphous. The poly(SA-FA) series displayed high crystallinity regardless of monomer concentration.

## Introduction

Bioerodible polymers have been used in a number of applications including biomaterials and drug carriers. The degradation process in these polymers is generally classified as either bulk or surface erosion. Surface erosion is achieved when the degradation occurs at the surface of the device and approaches the center in a predictable way. In contrast, bulk erosion is characterized by degradation that occurs simultaneously throughout the device. The type of erosion obtained is influenced by the intrinsic chemical properties of the polymer such as hydrophobicity and bond stability. Morphological characteristics of the polymer are also important factors in controlling erosion rates. Crystalline regions erode more slowly than amorphous regions,[1,2] and the type of crystals that form the crystalline region may affect the erosion rate. In polyanhydrides, the model polymer for this study, chemical properties such as bond stability, hydrophobicity, and degradation rate have been previously examined only to a limited extent.[3,4] A quantitative correlation between polyanhydride copolymer composition and device morphology has yet to be established.

In this paper we report the effect of copolymer composition on certain aspects of polyanhydride morphology. Polymers were characterized by differential scanning calorimetry (DSC) to yield thermal parameters such as glass transition temperature ($T_g$) and the melting point ($T_m$). Crystallinity was characterized with three different methods: (1) X-ray diffraction, (2) a combination of

* All correspondence should be addressed to Dr. R. Langer at MIT.
† Joint Center for Radiation Therapy, Harvard Medical School, Boston, MA 02115.

0024-9297/90/2223-3212$02.50/0 

X-ray diffraction and DSC, and (3) $^1$H NMR spectroscopy.[5] X-ray diffraction alone requires a clear separation of the amorphous halo from the crystalline pattern and could not be used to measure percent crystallinity for all the polymers that were studied. In cases where this defined separation did not exist, the second method provided an alternative way to determine percent crystallinity. The third method used $^1$H NMR spectroscopy data combined with Flory's equilibrium theory[6] to determine the theoretical minimum sequence length, $\xi$, which is needed for crystallization of specific copolymers. The results of crystallinity characterization as well as thermal analysis were then compared with sequence length distributions previously measured by $^1$H NMR.[5] As a consequence, a more complete picture relating polymer sequence distribution to morphological parameters such as percent crystallinity, $T_g$, $T_m$, and type of crystal within the crystalline region was obtained.

## Materials and Methods

**Polymer Synthesis.** Sebacic acid (SA), fumaric acid (FA), 4-hydroxybenzoic acid, 1,3-dibromopropane, and 5-bromovaleric acid were all purchased from Aldrich Chemical Co. The polyanhydrides were synthesized by melt polycondensation of mixed anhydrides of diacids and acetic acid. Poly(sebacic anhydride) (poly(SA)), poly[1,3-bis(*p*-carboxyphenoxy)propane] (poly(CPP)), poly(CPP-SA), poly[1,3-bis(*p*-carboxyphenoxy)-hexane] (poly(CPH)), poly(CPH-SA), and poly(fumaric anhydride) (poly(FA)) and copolymers of FA and SA were prepared according to the literature.[7,8]

**Experimental Procedures.** Infrared spectroscopy was performed on a FTIR spectrophotometer (Perkin-Elmer). Polymeric samples were film cast onto NaCl plates from a solution of the polymer in chloroform. The melting points of prepolymers were determined on a Fisher-Johns melting point apparatus. The molecular weights of polymers were estimated on a gel permeation chromatography (GPC) system (Perkin-Elmer) consisting of the Series 10 pump and the 3600 Data Station with the LKB 214 rapid spectral detector at 254 nm. Samples were eluted in chloroform (alcohol free) through a PLGel 5-$\mu$m mixed column (Polymer Laboratories) at a flow rate of 0.9 mL/min at 23 °C. Molecular weights of polymers were determined relative to polystyrene standards (Polysciences, molecular weight between 500 and 160 000) using CHROM 2 and GPC 4 computer programs (Perkin-Elmer). $^1$H NMR spectra were obtained on a Varian 270-MHz spectrophotometer using chloroform-$d_1$ as a solvent and tetramethylsilane (TMS) as an internal reference. Wide-angle X-ray powder diffraction of polymers in the form of pressed disks (1 mm thick) was recorded on a Rigaku RU300 Philips X-ray diffractometer using a nickel-filtered Cu K$\alpha$ source. The thermal properties of the polymers were determined on a DSC-7 differential scanning calorimeter (Perkin-Elmer) employing heating and cooling rates of 10 °C/min. Each sample was run at least twice. Heats of fusion were determined from the first run and the $T_g$ from the second run. All samples of soluble copolymers, for $^1$H NMR, were purified by dissolving in methylene chloride and quenching in *n*-hexane.

Insoluble polymers (homopolymers containing aromatic moieties and copolymers with a high percent of aromatic monomers) were cooled slowly from the melt and used without further purification. The same samples were used for both the X-ray powder diffraction and the DSC studies.

## Theoretical Background

**Determination of Polymer Compositions.** Copolymer composition was determined by $^1$H NMR spectroscopy by analyzing the ratio of the integration peaks at 1.3 ppm (8 H, sebacic) and those at 6.9–8.2 ppm (8 H, CPP or CPH). Mole fraction, $F_A$, was calculated from these integration curves.

**Copolymer Distribution and Average Sequence Length As Determined by NMR Spectroscopy.** $^1$H NMR spectra of poly(CPP-SA) or poly(CPH-SA) revealed two doublets at 8.1 and 8.0 ppm ($J$ = 8.7 Hz) and two triplets at 2.6 and 2.4 ppm ($J$ = 7.4 Hz).[5] For the homopolymers, poly(SA) has only one triplet at 2.4 ppm and poly(CPP) has only one doublet at 8.1 ppm. The downfield doublet, at 8.1 ppm, was the diad CPP–CPP, and the doublet at 8.0 ppm was the diad CPP–SA. Similarly, the upfield triplet, at 2.6 ppm, was the diad SA–CPP and the triplet at 2.4 ppm was SA–SA. By integration of the $^1$H NMR spectra, the following were calculated: (1) The *unconditional probabilities*, $P_{SA}$ and $P_{CPP}$, that a randomly selected monomer unit in the polymeric chain was either SA or CPP, which were determined by the overall integration ratio SA/CPP; (2) the *probabilities*, $P_{SA-SA}$, $P_{SA-CPP}$, and $P_{CPP-CPP}$, that a randomly selected diad was either SA–SA, SA–CPP, or CPP–CPP, which were determined from the integration ratios of the diads: SA–SA/SA–CPP (peaks at 2.4 and 2.6 ppm, respectively) and CPP–CPP/CPP–SA (peaks at 8.1 and 8.0 ppm, respectively). From these probabilities and the feed ratios we were able to calculate the following:[5] (1) the *conditional probability* of a chain ending with SA (or CPP) to add SA (or CPP) and (2) the number-average sequence length ($L_n$).[5]

**Calculation of Degree of Crystallinity.**

Crystallinity was determined from (a) X-ray powder diffraction and (b) the combination of both X-ray diffraction and DSC measurements.

For X-ray diffraction, the crystallinity is given by the equation

$$X'_c = A_c/(A_a + A_c) \quad (1)$$

where $X'_c$ is the percent crystallinity of the homopolymers, $A_a$ is the area under the amorphous hump, and $A_c$ is the area remaining under the crystalline peaks.[9,10] This was calculated for the poly(CPP-SA), poly(CPH-SA), and poly(FA-SA) series.

When X-ray diffraction and DSC measurements were used, the relative degree of crystallinity of the copolymers was calculated from the crystallinity of the homopolymers. The fraction of crystallites estimated from X-ray diffraction is 61% for poly(CPP) and 67% for poly(SA). For each copolymer (with m1 and m2 the monomers in each copolymer), the degree of crystallinity is defined as

$$X_c = \Delta H_{obs}/(W_{m1}\,\Delta H_{m1,pure} + W_{m2}\,\Delta H_{m2,pure}) \quad (2)$$

where $X_c$ is the percent crystallinity of the copolymers, $\Delta H_{obs}$ is the heat of fusion in calories per gram for each copolymer, $W_{m1}$ and $W_{m2}$ are the weight fractions of the monomers in each copolymer and

$$\Delta H_{i,pure} = \Delta H_{i,obs}/X'_{i,c} \quad i = m1, m2 \ldots \quad (3)$$

where $X'_{i,c}$ was determined for each homopolymer from eq 1. Molar weights for the monomer units were 192, 410, 454, and 198 g/mol for SA, CPP, CPH, and FA, respectively. $\Delta H_{pure}$ was 52.9 and 43.6 cal/g for poly(SA) and poly(CPP), respectively. This type of calculation was chosen since the two monomers form crystalline homopolymers. For general applications the maximum crystallizability is referred to as 100% crystallinity of one the homopolymers. In the calculations, the denominator of eq 2 expresses the *crystallizability* for each copolymer. This crystallizability is determined by the chemical structure of the polymer and in practice may never be achieved since the entire polymer may not be 100% crystallizable. The *crystallinity*, which is given by eqs 1 and 2, is a property of the physical conditions of crystallization,

details for which were presented in Experimental Procedures.

**Equilibrium Theory of Crystallization.** Flory[6] demonstrated that near the melting point, polymer crystals and amorphous material should exist in thermodynamic equilibrium. A complete theoretical treatment has been made on those cases of A–B copolymers in which only the A unit is capable of entering into the crystalline lattice. This is not the case in all of our copolymers, but this treatment is still valid within certain limits as discussed below. In the molten state, crystallizable A units occur in a defined distribution of sequence lengths determined by copolymer composition. In a crystallized polymer there will also be a distribution of crystal lengths determined by the copolymer composition. Therefore, in a crystallized polymer, there will be a distribution of crystalline lengths, $\xi$, of repeating A units in a single chain running from one end of the crystallite to the other. Longitudinal growth of crystallites will be restricted by the presence of B units, which occur at the crystallites. Lateral growth is restricted by the availability of A units in the amorphous region. In order to use Flory's model, it is assumed that, as CPP monomer is added to the SA monomer, it restricts the growth of the SA units. Similarly, when SA is added to the CPP monomer it restricts the growth of CPP units. In the case of SA and CPH the system fits the model since poly(CPH) displays an amorphous structure (as discussed later). Prior to development of any crystallinity, the distribution of A sequences in the melt is determined by[6]

$$W_\xi^\circ = \xi(F_A/P_{AA})(1 - P_{AA})^2 P_{AA}\xi \qquad (4)$$

where $W_\xi^\circ$ is the weight fraction of sequences present that are exactly $\xi_A$ units long, $P_{AA}$ (this is $P_{SA\text{-}SA}$ or $P_{CPP\text{-}CPP}$ according to the NMR model) is the probability that an A unit is followed immediately by another A unit, independent of the number of preceding A units in the chain, and $F_A$ is the mole fraction of A units in the copolymer. $F_A$ is also the maximum crystallizability for each copolymer. As the temperature is lowered the longest sequences tend to crystallize first followed by the shortest ones. If $\xi^*$ is the minimum sequence length that melts at temperature $T$, the maximum crystallinity at this temperature is achieved when all $\xi^*$ are longer crystallized. The crystallizability, $W_c$, is

$$W_c = (F_A/P_{AA})P_{AA}\xi^*[\xi^*(1 - P_{AA}) + P_{AA}] \qquad (5)$$

Equation 6 is used in order to determine $\xi^*$, using $W_c$ that was calculated according to eq 1; $F_A$ and $P_{AA}$ are calculated from the $^1$H NMR results as described earlier.

**Calculation of Crystallite Size from Broadening of the Diffraction Pattern.** When the Scherrer and Bragg approximation[11] was used, the size of crystallites was determined as

$$\beta = K\lambda/(t \cos \Theta) \qquad (6)$$

where $\beta$ is the half-width of the diffraction function, $\lambda$ is the wavelength of the X-ray, $t$ is the crystallite size, $\Theta$ is the Bragg angle, and $K$ is the Scherrer constant and has a value of 0.94.[11]

## Results and Discussion

**Polymer Characterization.** All the polyanhydrides were analyzed by GPC. Molecular weights (W.A.) for the poly(CPP–SA), poly(PCH–SA), and poly(FA–SA) series were 50 000–100 000, 20 000–40 000, and 4000–25 000, respectively. IR spectral analysis of poly(CPP–SA) and poly(CPH–SA) copolymers revealed typical anhydride absorbances at 1720 and 1780 cm$^{-1}$. IR spectra of poly(FA) revealed bonds at 1780 and 1740 cm$^{-1}$, characteristic for conjugated noncyclic anhydrides, and an olefinic stretch at 3080 cm$^{-1}$.[12]

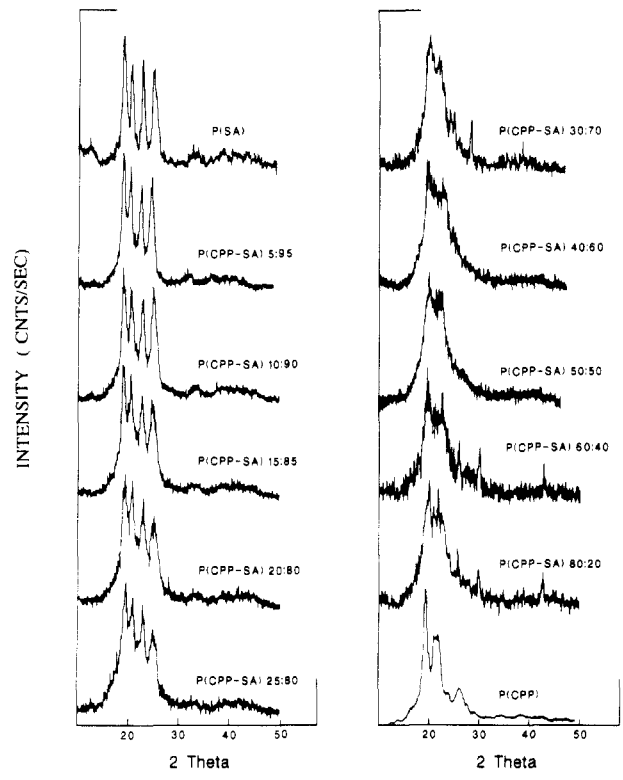


**Figure 1.** X-ray powder diffraction of the P(CPP–SA) series. ($2\theta$ indicates the diffraction angle).

**X-ray Diffraction Patterns of Homo- and Copolymers.** The propensity of a copolymer to crystallize depends on whether the monomer units are three-dimensional, similar in shape and size, and on the differences between the lateral dimensions of the molecule chains. A good example of two monomers of similar size are styrene and *o*-fluorostyrene.[10] There are a variety of diffraction patterns displayed by their homo- and copolymers:[10] (1) The crystalline diffraction pattern of the homopolymer of one component may be very distinct, (2) the diffraction pattern of a homopolymer of A and B may be superimposed, (3) a new diffraction pattern, distinct from the homopolymer of either component, may appear, and (4) the crystallinity may disappear, whereupon the pattern will consist entirely of amorphous diffraction halos.

Crystallinity is strongly affected by other factors including the properties of monomers A and B, the mutual affinities of the monomer units of A and B (mutual solubilities), in any differences in the crystallinities of the homopolymers A and B, and in the incidence of blocks of either A and B. In the following discussion we will address all of these points while characterizing three types of copolymers.

**(a) Poly(CPP–SA) Copolymers.** Figure 1 displays the X-ray powder diffraction of the poly(SA) and poly(CPP) homopolymers and the poly(CPP–SA) copolymer series. At the top of the figure the distinct structure related to the poly(SA) homopolymer is revealed. It is characterized by four peaks at 4.41, 4.10, 3.72, and 3.42 Å; their respective crystallite sizes are 6.8, 10.4, 13.6, and 3.7 Å. Crystal size was determined from eq 7 (see also Table IA). Powder diffraction of the poly(CPP) homopolymer

**Table I**

A. X-ray Diffraction and Crystallite Size of Poly(CPP-SA) Copolymers[a]

| polymer | X-ray diffractions in decreasing order | | | | |
|---|---|---|---|---|---|
| poly(SA), 100% | 4.41 (6.8) | 4.1 (10.4) | 3.72 (13.6) | 3.42 (3.7) | |
| poly(CPP-SA), 4:96 | 4.66 (5.9) | 4.3 (7.2) | 3.89 (9.4) | 3.55 (8.4) | |
| poly(CPP-SA), 9:91 | 4.62 (5.8) | 4.28 (5.9) | 3.88 (7.9) | 3.55 (0.2) | |
| poly(CPP-SA), 87:13 | 4.66 (3.4) | 4.3 (4.9) | 3.89 (6.43) | 3.57 (6.2) | |
| poly(CPP-SA), 17:83 | 4.64 (4.9) | 4.33 (4.81) | 3.89 (4.2) | 3.57 (6.2) | |
| poly(CPP), 100% | 4.64 (7.9) | 4.15 (9.4) | 4.0 (9.4) | 3.58 | 3.24 |

B. Heat of Fusion and Crystallinity of Poly(CPP-SA)[b]

| polymer | $T_m$, °C | $T_g$, °C | heat of fusion, cal/g | crystallinity $X_c$, % | crystallinity $W_c$, % |
|---|---|---|---|---|---|
| poly(SA), 100% | 86.0 | 60.1 | 36.6 | | 66.0 |
| poly(CPP-SA), 4:96 | 76.0 | 41.7 | 24.9 | 46.5 | 58.7 |
| poly(CPP-SA), 9:91 | 78.0 | | 25.7 | 48.5 | 47.8 |
| poly(CPP-SA), 13:87 | 75.0 | 47.0 | 20.7 | 39.5 | 40.5 |
| poly(CPP-SA), 17:83 | 72.0 | 47.0 | 19.3 | 37.0 | 40.2 |
| poly(CPP-SA), 22:78 | 66.0 | 47.0 | 15.3 | 30.0 | 35.0 |
| poly(CPP-SA), 27:73 | 66.0 | 44.0 | 10.2 | 20.0 | 16.2 |
| poly(CPP-SA), 31:69 | 66.0 | 40.0 | 5.1 | 10.6 | 14.5 |
| poly(CPP-SA), 41:59 | 178.0 | 4.2 | 2.0 | 4.0 | 16.2 |
| poly(CPP-SA), 46:54 | 185.0 | 1.8 | 3.1 | 6.1 | 14.2 |
| poly(CPP-SA), 60:40 | 200.0 | 0.2 | 6.0 | 13.9 | 15.0 |
| poly(CPP-SA), 80:20 | 205.0 | 15.0 | 8.2 | 17.6 | 19.5 |
| poly(CPP), 100% | 240.0 | 96.0 | 26.5 | | 61.4 |

C. Comparison between the Number-Average Sequence Length ($L_n$) and the Minimum Sequence Length ($\xi^*$) for the Poly(CPP-SA) Series

| polymer | $F_A$, mol % | $P_{AA}$, mol % | $L_n$ (SA) | $\xi^*$ |
|---|---|---|---|---|
| P(CPP-SA), 96:4 | 0.96 | 0.86 | 12.3 | 9.10 |
| P(CPP-SA), 91:9 | 0.91 | 0.77 | 8.6 | 6.65 |
| P(CPP-SA), 87:13 | 0.87 | 0.68 | 6.8 | 5.28 |
| P(CPP-SA), 83:17 | 0.83 | 0.61 | 5.6 | 5.20 |
| P(CPP-SA), 78:22 | 0.78 | 0.64 | 5.1 | 4.69 |
| P(CPP-SA), 59:41 | 0.59 | 0.35 | 2.5 | 3.03 |
| P(CPP-SA), 56:44 | 0.56 | 0.29 | 2.3 | 1.90 |

[a] Diffraction given in angstroms; numbers in parentheses indicate the crystal size corresponding to the specific diffraction. [b] In a few cases it was difficult to determine the $T_g$, and blank spaces are left.

is shown at the bottom right of Figure 1. Again it is characterized by a well-defined pattern at 4.64, 4.15, 4.0, 3.58, and 3.24 Å; crystal sizes of 7.9 and 9.4 Å were found for the first two diffractions (the other peaks were too wide to be determined by eq 7) (Table IA). As the percent of CPP is increased, there is a change in the diffraction pattern, especially near a 30:70 ratio of CPP/SA in the copolymer. Up to this concentration the defined structures corresponding to the poly(SA) crystallites are easily recognized (Figure 1). Above 30% CPP, the crystalline structure disappears and the pattern consists entirely of an amorphous structure. As the concentration of the CPP is further increased, the typical structure of the poly(CPP) homopolymer appears again (above 70% CPP). From this study it seems that crystallite structures are determined mostly by the monomer with the highest concentration in the copolymer. This property is of great importance, especially in studying erosion phenomena in polymers; crystalline regions will erode more slowly than amorphous regions,[2] and the *type of crystals* that form

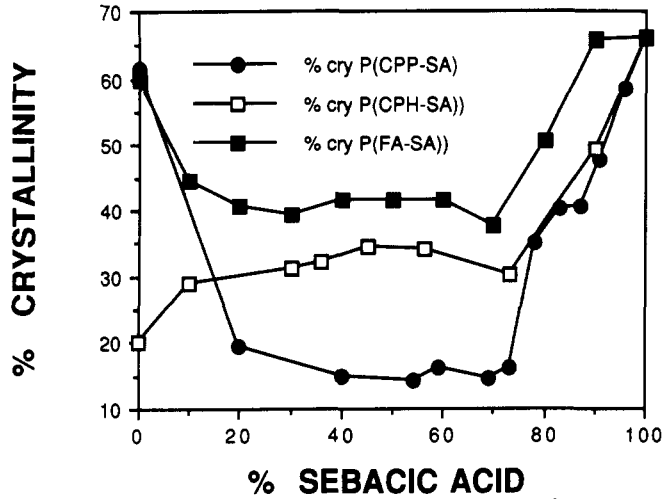


**Figure 2.** Percent crystallinity of P(CPP-SA), P(CPH-SA), and P(FA-SA) polymers.

the crystalline region may determine the erosion rate.

Table IB summarizes some physical properties of the poly(CPP-SA) copolymers. By DSC the melting point, $T_m$, and the glass transition, $T_g$, of the copolymer series were detected. Copolymers display a typical melting point behavior, as also predicted by Flory.[6] The melting point of poly(SA) was 86 °C, and the $T_g$ was 60 °C. As CPP monomer was increased, the melting point decreased to a minimum around 30% CPP and gradually increased to 240 °C for the poly(CPP) homopolymer (Table IB). The $T_g$ of poly(CPP) was 96 °C as was found by others.[13] However, as can be seen from Table IB, there was a concave relation between $T_g$ and percent sebacic acid with a minimum in $T_g$ near a 50:50 monomer ratio of CPP/SA. This behavior deviates from the linear relation predicted by the DiMarzio-Gibbs equation.[14] Similar deviations were obtained with other polymer systems.[15]

Heat of fusion values for the polymers demonstrate a dramatic decrease as CPP is added to SA, or vice versa. Heat of fusion was minimal for the 50:50 copolymers. Flory[6] demonstrated that when a noncrystallizable unit is introduced into a crystallizable monomer, a decrease in crystallinity will occur. In our case, the decrease of crystallinity is a direct result of the random presence of these units in the polymer chain.[5] This randomness makes crystallization more difficult, especially when the lateral and three-dimensional sizes of the two monomers, CPP and SA, are very different. Table IB and Figure 2 summarize the crystallinities of the homo- and copolymer series as determined by X-ray powder diffraction and eq 1. Since this method is useful only for cases where the diffraction patterns are well-defined, we developed a second method (see eq 2 in Theoretical Background) using both DSC and X-ray powder diffraction for the determination of crystallinity ($X_c$). The trend of decreasing crystallinity, as one of the monomers is added, appeared by using both of these methods. The two methods give similar results, except for the more amorphous polymers, where determination of the amorphous area is more difficult. However, for the more amorphous polymers the method using both DSC and X-ray diffraction is probably more reliable. This is true as long as $\Delta H_{pure}$ is easily determined for both homopolymers. As we shall see, this is not always the case with some of the polyanhydrides. At this point it is important to notice the correlation between an earlier study[5] made with $^1$H NMR and the present study. It was recognized by $^1$H NMR that, up to a 25:75 ratio of either CPP/SA or SA/CPP, the polymer had a blocklike distribution. The number-average sequence length

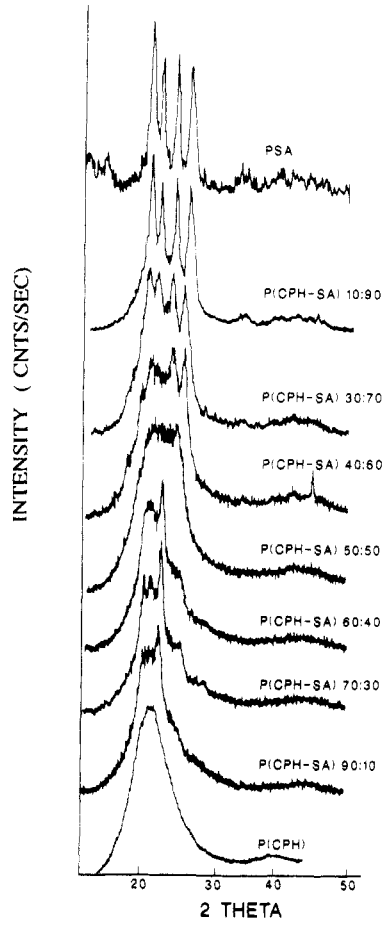


**Figure 3.** X-ray powder diffraction of the P(CPH-SA) series. ($2\theta$ indicates the diffraction angle).

($L_{SA}$) of sebacic acid decreased from 8 to 2 for the poly(CPP-SA) series starting with a CPP/SA ratio of 5:95 and progressing to a CPP/SA ratio of 50:50.[3]

In order to further study this correlation, we solved eq 6 (graphically). By using the probabilities ($F_A$ and $P_{AA}$), which were obtained by NMR,[3] and the degrees of crystallinity, which were obtained by the X-ray diffraction, we could determine $\xi^*$, the minimum sequence length, which melts at the temperature $T$ (for details see Theoretical Background). Results are summarized in Table IC. The values that were obtained for $\xi^*$ are similar to $L_n$ (the average sequence length) values, which were obtained by $^1$H NMR[5] (Table IC), except for the high concentration of SA where $\xi^*$ was slightly smaller than $L_n$ that was obtained by $^1$H NMR. At higher SA concentrations, the polymer does not behave like a random copolymer.[5] The use of $^1$H NMR probabilities to obtain $\xi^*$ was possible only for those polymers that were soluble in organic solvents (since polymers made from CPP/SA with mole ratios higher than 50:50 are not soluble in organic solvents, they were not studied by NMR).

**(b) Poly(CPH-SA) Copolymers.** Figure 3 displays powder diffraction of the poly(SA) and poly(CPH) homopolymers and the poly(CPH-SA) copolymers. At the top of the figure the distinct structure related to poly(SA) is seen again. At the bottom, the amorphous halo of the poly(CPH) polymer is displayed. In this case we actually have two homopolymers: one is crystalline (poly(SA)); the other is not (poly(CPH)). The general tendency of the defined structure of the poly(SA) to disappear, as the amount of CPH is added, is repeated. Again, after 30% CPH is added, a broad halo appears, on the top of which some fine diffraction still persists. Crystal size was not determined for the series, since the peaks were too broad for eq 6 to apply.

Table IIA displays the melting points and the glass transition temperatures of the poly(CPH-SA) series. The melting point of poly(CPH) is lower than poly(CPP), which is consistent with previous studies.[13] This low melting point of the homopolymer enables copolymers to be obtained with decreasing melting points, to a minimum of 43-49 °C around 50:50 and 60:40 CPH/SA ratios (see Table IIA). This fact is of great practical importance, particularly because these polymers are subjected to different formulation procedures (e.g., for use inn biomaterials or controlled release systems) in the vicinity of the melting points (e.g., injection molding or hot melt encapsulation[3,16]). Obtaining polymers with low melting points is important for successful formulation using these procedures, since they may enable the development of procedures in which polymer-drug systems are fabricated at temperatures that are low enough to prevent drug decomposition or polymer-drug interaction during fabrication. The glass transition is around 60 °C for poly(SA) and decreases as CPH is added. For instance, a 50:50 copolymer has a $T_g$ of 11.5 °C, which means that at room temperature the polymer is in its rubbery state. The same concave relation (as in the P(CPP-SA) series) between $T_g$ and percent sebacic acid in the P(CPH-SA) series was obtained.

The heat of fusion decreases from 36.6 cal/g for poly(SA) to 2.5 cal/g for the 50:50 copolymer. A slight increase in heat of fusion was observed when the ratio of CPH was increased (Table IIA). The heat of fusion for poly(CPH) was very low (1.7 cal/g) and with its halo diffraction, it was difficult to obtain its $\Delta H_{a,pure}$. For this reason, crystallinity was determined only by X-ray powder diffraction. There was a decrease in crystallinity as the concentration of CPH increased, but in contrast to the poly(CPP-SA) series, the crystallinity was much higher for the poly(CPH-SA) copolymers between mole ratios of CPH/SA 30:70 to 70:30 (Table IIA).

The polymers in the poly(CPH-SA) series were more soluble in common NMR solvents, and this is why it was possible to study the entire series.[5] Table IIB summarizes the data obtained from NMR. Up to a ratio of 25:75 of either CPH/SA or SA/CPH, the polymer had a block-type distribution. The number-average sequence length ($L_{SA}$) decreased from 6 to 2 for the poly(CPH-SA) series (from 10:90 to 50:50). Using the unconditional probabilities $P_{SA-SA}$ for high ratios of SA (up to 50:50 ratios) and $P_{CPH-CPH}$ for higher concentrations of CPH, $\xi^*$ was calculated using eq 5. The numbers for $\xi^*$, which are listed in Table IIB, closely correlate with $L_{SA}$ and $L_{CPP}$ obtained by $^1$H NMR. The correlation that was obtained for both the CPP-SA and CPH-SA series enabled the use of eq 5 in order to predict crystallinity of polyanhydrides using just NMR spectra. That is by obtaining $L_n$ and $P_{SA-SA}$ from $^1$H NMR and solving eq 5, one can obtain a good estimation of the degree of crystallinity.

**(c) Poly(FA-SA) Series.** The last series studied, poly(FA-SA), revealed an interesting powder diffraction (Figure 4). The crystalline poly(SA) and its four typical diffractions are presented at the top left side. The three diffractions of poly(FA) at 4.09, 3.70, and 3.14 Å with crystal sizes of 10.37, 9.10, and 20.47 Å, respectively, are shown in the lower right side (see also Table IIIA). In this particular case, both homopolymers are crystalline. The copolymers display a typical poly(SA) diffraction up to 20:80 FA/SA ratios. Above ratios of 30:70 SA/FA, a new diffraction appears at 4.28, 3.98, and 3.64 Å. The biggest crystal sizes were found for the poly(FA-SA) series,

**Table II**

A. Heat of Fusion and Crystallinity of Poly(CPH-SA)

| polymer | $T_m$, °C | $T_g$, °C | heat of fusion, cal/g | crystallinity $W_c$, % |
|---|---|---|---|---|
| poly(SA), 100% | 86.0 | 60 | 36.6 | 66.0 |
| poly(CPH-SA), 10:90 | 74.4 | 58.3 | 17.8 | 49.4 |
| poly(CPH-SA), 18:82 | 66.4 | | 13.1 | |
| poly(CPH-SA), 27:73 | 57.2 | 45.0 | 9.3 | 30.2 |
| poly(CPH-SA), 44:56 | 52.7 | 6.1 | 7.2 | 34.5 |
| poly(CPH-SA), 55:45 | 49.5 | 11.5 | 3.2 | 34.4 |
| poly(CPH-SA), 64:36 | 43.3 | 11.8 | 2.5 | 32.1 |
| poly(CPH-SA), 70:30 | 110.5 | 14.5 | 3.0 | 31.2 |
| poly(CPH-SA), 80:20 | 133.1 | 34.8 | 7.3 | |
| poly(CPH-SA), 90:10 | 136.2 | 26.0 | 18.7 | 28.8 |
| poly(CPH), 100% | 143.1 | 47 | 1.7 | 20.0 |

B. Comparison between the Number-Average Sequence Length ($L_n$) and Minimum Sequence Length ($\xi^*$) for the Poly(CPH-SA) Series[a]

| | $L_n$ | | | | | | |
|---|---|---|---|---|---|---|---|
| polymer | $F_A$ | $F_B$ | $P_{AA}$ | $P_{BB}$ | SA | CPP | $\xi^*$, Å |
| poly(CPH-SA), 18:82 | 0.82 | | 0.68 | | 5.6 | | 5.53 |
| poly(CPH-SA), 27:73 | 0.73 | | 0.53 | | 3.7 | | 3.77 |
| poly(CPH-SA), 37:63 | 0.63 | | 0.40 | | 2.7 | | 2.35 |
| poly(CPH-SA), 44:56 | 0.56 | | 0.32 | | 2.3 | | 2.11 |
| poly(CPH-SA), 55:45 | 0.45 | | 0.29 | | 1.8 | | 1.72 |
| poly(CPH-SA), 64:36 | | 0.64 | | 0.39 | | 2.6 | 2.44 |
| poly(CPH-SA), 80:20 | | 0.83 | | 0.67 | | 5.0 | 6.25 |
| poly(CPH-SA), 85:15 | | 0.85 | | 0.70 | | 5.7 | 6.38 |

[a] $F_A$, $F_B$, $P_{AA}$, and $P_{BB}$ are given in mole fraction.

**Table III**

A. X-ray Diffraction and Crystallite Size of P(CPP-SA) Copolymers[a]

| polymer | X-ray diffractions in decreasing order | | | | | |
|---|---|---|---|---|---|---|
| PFA, 100% | 4.09 (10.37) | 3.7 (9.1) | 3.14 (20.47) | | | |
| P(FA-SA), 90:10 | 4.11 (7.76) | 3.86 (78.6) | 3.14 (19.6) | | | |
| P(FA-SA), 80:20 | 4.33 | 4.11 | 3.89 | 3.67 | 3.62 | 3.30 |
| P(FA-SA), 70:30 | 4.32 | 4.10 | 3.89 | | | |
| P(FA-SA), 60:40 | 4.26 (3.47) | 3.88 (4.2) | 3.55 (7.2) | | | |
| P(FA-SA), 50:50 | 4.28 (3.3) | 3.95 (5.4) | 3.6 (14.2) | | | |
| P(FA-SA), 40:60 | 4.33 (4) | 3.98 (7.9) | 3.64 (12.13) | | | |
| P(FA-SA), 30:70 | 4.48 | 4.18 | 3.95 | 3.55 (5.9) | | |
| P(FA-SA), 20:80 | 4.41 (5.4) | 4.14 (5.25) | 3.73 (7.62) | 3.41 (7.33) | | |
| P(FA-SA), 10:90 | 4.39 (5.410 | 4.11 (4.5) | 3.57 (2.8) | 3.39 (3.3) | | |
| P(SA), 100% | 4.43 (6.8) | 4.15 (10.4) | 3.75 (13.56) | 3.45 (3.7) | | |

B. Heat of Fusion and Crystallinity of Poly(FA-SA)[b]

| polymer | $T_{m1}$, °C | $T_{m2}$, °C | $T_g$, °C | fusion cal/g | crystallinity $W_c$, % |
|---|---|---|---|---|---|
| PFA, 100% | 246.2 | | 41.2 | 16.00 | 60 |
| P(FA-SA), 90:10 | 213 | | 56.0 | 13.8 | 44.5 |
| P(FA-SA), 80:20 | 185.7 | | 58 | 22.78 | 40.7 |
| P(FA-SA), 70:30 | 106 | 157.8 | 46 | 5.7 (4.5) | 39.2 |
| P(FA-SA), 60:40 | 94.7 | 144 | | 4.7 (4.9) | 41.7 |
| P(FA-SA), 50:50 | 69 | 100 | | 12.5 (7.0) | 41.6 |
| P(FA-SA), 40:60 | 68 | 91 | 47 | 9.0 (8.4) | 41.6 |
| P(FA-SA), 30:70 | 67 | 91 | 46 | 7.9 (13.8) | 37.6 |
| P(FA-SA), 20:80 | 73.9 | 86 | | 21.9 | 50.6 |
| P(FA-SA), 10:90 | 83 | | 55 | 25.8 | 65.8 |
| P(SA), 100% | 86 | | 60 | 36.6 | 66.0 |

[a] Diffraction is given in angstroms; numbers in parentheses indicate the crystallite size corresponding to the specific diffraction. [b] Blanks indicate cases where $T_g$ or $T_m$ was not observed.

with sizes ranging from 4 to 20 Å (Table IIIA). As the FA concentration increased above 80% fumaric acid, the defined structure of poly(FA) reappears. Crystal type is again determined by the monomer with the higher concentration in the copolymer. However, at a 50:50 ratio of FA/SA the copolymers display a very crystalline structure, and new diffractions at 4.28, 3.95, and 3.6 Å appeared. This structure can be attributed to the type of copolymer that was formed. In earlier studies, we described[5,8] that the 50:50 copolymers were actually arranged in an alternating dimer structure. By using $^1$H NMR spectroscopy data, it was possible to show that the following order FA-FA-SA-SA-FA-FA...[8] actually exists. These organized alternating dimers may lead to the new diffraction pattern. The results here are different than what was shown for the previous copolymers, poly(CPP-SA) and poly(CPH-SA), at the same mole ratio. Since the two monomers, FA and SA, are quite similar in size, they do not interfere with crystallite formation. In contrast, in both copolymers of poly(CPP-SA) 50:50 and poly(CPH-SA) 50:50, amorphous structures appear in spite of the same alternating structure that was found by $^1$H NMR

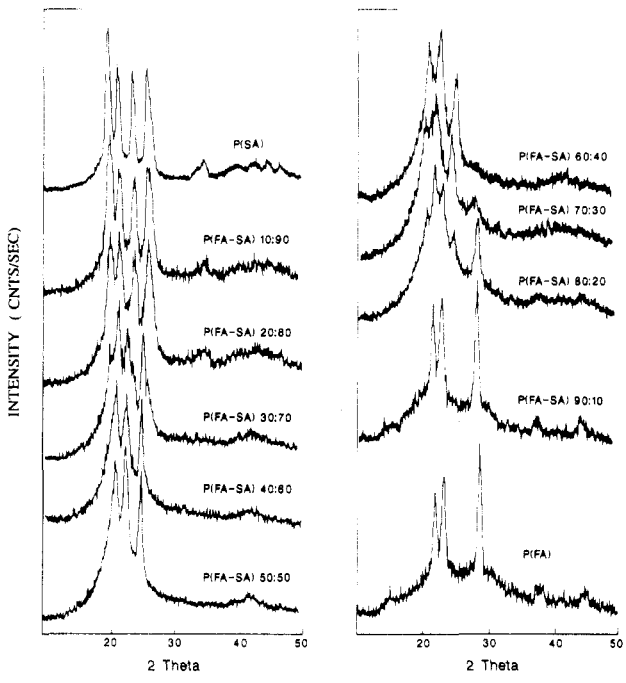


**Figure 4.** X-ray powder diffraction of the P(FA–SA) series. ($2\theta$ indicates the diffraction angle).

studies.[5] The reason for this behavior could be the differences between the sizes of the SA and CPP and the SA and CPH monomers.

Table IIIB summarizes the physical properties of the polymers. The melting point decreases as SA is added to poly(FA) from 246.2 to 86 °C. The $T_g$ for most of the polymers was between 40 and 56 °C, which means that at room temperature the polymers are in their glassy state. Copolymers made of 70:30 FA–SA and higher concentrations of FA revealed two melts (Table IIIB). This phenomenon is under investigation and may be attributed to two types of crystals that exist in the melt. The fact that we have two melts introduces a slight difficulty in calculating the crystallinity using both DSC and X-ray diffraction. In this case, the crystallinity was determined by the X-ray diffraction pattern only. The change in crystallinity throughout the series was not so extreme and no dramatic decrease was obtained near a 50:50 monomer ratio of FA–SA; actually, between a 90:10 and 30:70 mole ratio of FA–SA, the crystallinity remained almost the same (~40%) (the crystallinity of the CPP/SA or CPH/SA series close to a 50:50 monomer ratio, displayed a decrease in crystallinity as compared to the homopolymers). This high degree of crystallinity may be one of the reasons for achieving good surface erosion with these particular polymers.[17]

Several papers have been published on polyanhydrides in an attempt to correlate physicochemical properties of polyanhydrides to their erosion rates.[1,5,16,17] This is the first such study to examine crystallinity, one of the most important properties that contributes to erosion processes.

In the current study a series of polyanhydrides were characterized in terms of crystallinity via DSC, X-ray powder diffraction, and $^1$H NMR. The methods used enabled the determination of the crystallinity of a variety of polyanhydride copolymers and the correlation of these results with sequence length distributions as measured by NMR. It was found that crystallinity is predominantly determined by the monomer with the higher percentage in the copolymers. At higher ratios of SA in both poly(CPP–SA) and poly(CPH–SA) copolymers, $^1$H NMR revealed long sequence lengths and a block-type structure. X-ray results revealed that crystallinity is determined by the SA units. In addition, calculating the minimum sequence length needed for crystallization, by using Flory's theory, yields similar results to the sequence length distribution, which was calculated independently by $^1$H NMR. As a result, $^1$H NMR data can be used to calculate degree of crystallinity without the use of X-ray diffraction.

## References and Notes

(1) Mendelkern, L. *Crystallization of polymers*; McGraw-Hill: New York, 1964.
(2) Ward, I. M. *Structure and properties of oriented polymers*; Applied Science Publishers Ltd.: London, 1982.
(3) Leong, K. W.; Brott, B. C.; Langer, R. *J. Biomed. Mater. Res.* **1985**, *19*, 941–955.
(4) Mathiowitz, E.; Saltzman, W. M.; Domb, A.; Dor, Ph.; Langer, R.; *J. Appl. Polym. Sci.* **1988**, *35*, 755–774.
(5) Ron, E.; Mathiowitz, E.; Mathiowitz, G.; Langer, R., submitted for publication in *Macromolecules*.
(6) Flory, J. P. *J. Chem. Phys.* **1949**, *17*, 223–240.
(7) Domb, A. J.; Langer, R. *J. Polym. Sci.* **1987**, *25*, 3373–3386.
(8) Domb, A.; Mathiowitz, E.; Ron, E.; Langer, R. submitted for publication in *J. Polym. Sci.*
(9) Young, R. J. *Introduction to Polymers*; Chapman and Hall: London, New York, 1981; p 224.
(10) Kakudo, M.; Kasai, N. *X-ray Diffraction by polymers*; Elsevier Publishing Co.: New York, 1972.
(11) Fava, R. A., Ed. *Methods of Experimental Physics, crystal structure and morphology*; Academic Press: New York, 1980; Vol. 16, Part B, p 128.
(12) Silverstein, R. M.; Bassler, G. C. *Spectrometric Identification of Organic Compounds*; John Wiley & Sons: New York, 1981; p 124.
(13) Conix, A. *J. Polym. Sci.* **1958**, *29*, 343–351.
(14) DiMarzio, E. A.; Gibbs, J. H. *J. Polym. Sci.* **1958**, *40*, 121.
(15) Hidematsu, S.; Mathot, B. F. *Macromolecules* **1989**, *22*, 1380–1384.
(16) Mathiowitz, E.; Langer, R. *J. Controlled Release* **1987**, *5*, 13–22.
(17) Mathiowitz, E.; Bernstein, H.; Langer, R. *Proc. Intl. Symp. Controlled Release Bioactive Mater.* **1989**, *16*, 161.